# Mechatronic track guidance on disturbed track: the trade-off between actuator performance and wheel wear[1]

Bernhard Kurzeck[2], Andreas Heckmann, Christoph Wesseler and Matthias Rapp

*Institute of System Dynamics and Control, German Aerospace Center (DLR), Oberpfaffenhofen, Muenchner Strasse, 20 82234 Wessling, Germany*

**Abstract**

Future high speed trains are the main focus of the DLR research project Next Generation Train (NGT). One central point of the research activities is the development of a mechatronic track guidance for the two axle intermediate wagons with steerable, individually powered, independently rotating wheels. The traction motors hereby fulfil two functions; they concurrently are traction drives and steering actuators. In this paper, the influence of the track properties – line layout and track irregularities – on the performance requirements for the guidance actuator is investigated using multi-body-models in SIMPACK®. In order to compromise on the design conflict between low wheel wear and low steering torques, the control parameters of the mechatronic track guidance are optimized using the DLR in-house software MOPS. Besides of the track irregularities especially the increasing inclination at transition curves defines high actuator requirements due to gyroscopic effects at high speed. After introducing a limiter for the actuating variables into the control system a good performance is achieved.

**Keywords:** Railway Dynamics, Track Guidance, Mechatronics, Control, Independently Rotating Wheels, Wear

## 1. Introduction

Independently rotating wheels (IRWs) offer new possibilities for designing efficient and lightweight rail vehicles. In addition, unnecessary creep in the wheel–rail contact is avoided by actively steered IRWs. Therefore, wheel and rail wear as well as noise emission can be significantly reduced. In the research project ‘Next Generation Train’ (NGT, Figure 1), DLR is developing a concept for a double-decker electric multiple unit for high-speed services with 400 km/h. This project is an internal research project which concentrates the different rail vehicle research activities of several DLR Institutes in one innovative train concept. Besides the running dynamics and mechatronic track guidance, other research topics are more energy efficiency by aerodynamic optimisation and by light weight construction, reduced sound emission, reduced life cycle costs and high passenger comfort. The concept includes two-axle intermediate wagons, which have single-axle running gears with IRWs. Each wheel is separately powered why this concept meets the definition of Driven Independently Rotating Wheels in [1]. Additionally, the pairs of IRW are assembled to an axle with a rotational degree of freedom around the vertical axis relative to the car body to allow perfect radial steering.

[1] This is an Authors’ Accepted Version of an article published in *Vehicle System Dynamics : International Journal of Vehicle Mechanics and Mobility*, *52:sup1*, *109-124*, 2014, DOI: 10.1080/00423114.2014.881514.

[2] Corresponding author. Email: bernhard.kurzeck@dlr.de

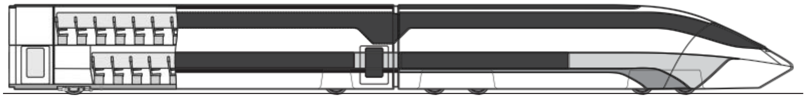

Figure 1. Side view of the NGT with leading train head and the first intermediate coach.

The mechatronic track-guidance contains a control system, which enables centring in the track and active radial steering for IRW pairs during curve passing. The wheel wear and noise generation can thus be considerably reduced. As far as advantages are concerned, the system offers the multi-functional use of the traction motors for traction, braking and track guidance tasks [2,3] and the compatibility with low floor concepts: In the NGT, continuous floors on both levels allow the passengers to easily walk through the train on both decks. In combination with an aerodynamically optimised train shape and lightweight structures, the train concept offers 75% more seats per length unit and 50% less energy consumption per seat compared to a conventional single-decker high-speed train at the same running velocity. The train concept is a proposal for a sustainable and highly efficient train of the future, because it offers a higher capacity in combination with reduced energy consumption, which is an important contribution on the way to a zero emission transportation sector.

*Bruni* et al. nominated three distinguished active concepts in their 2007 IAVSD state-of-the-art paper [4]: active primary suspensions, including the proposed mechatronic track guidance, active secondary suspensions and tilting. They concluded that for active primary suspensions '… that the prospective rewards for the railway system as whole are much larger than for active secondary suspensions – probably larger than for tilt …', but also that '… active suspensions applied to running gear are undoubtedly the most challenging to introduce …' This demonstrates the importance of such a system within an innovative train concept, but also that there are many research tasks. Therefore, several researcher teams have worked or currently are working in this field, e.g.[4–8] The mechatronic track guidance is a further development of the mechatronic wheelset.[3]

Because of their special design, the running behaviour of the NGT intermediate wagons (Figure 1) is in the main focus. These are two axle vehicles with four IRWs. The intermediate wagons of the NGT have a large axle distance of 14 m which requires an active radial steering in curves in order to ensure low wheel wear. In contrast, the running gears of the train heads have four IRWs because they have to carry more traction equipment and are more similar to a bogie. Because of the smaller axle distance in the bogie, lower steering angles are needed for radial steering. Therefore, the control of the intermediate coaches is more challenging and this is the reason for the presentation in this paper.

The general feasibility of the mechatronic track guidance system also for a high-speed application and the advantages on the wheel wear were shown in [2] using multi-body simulations. But the preliminary controller used in [2] unfortunately exposes high-frequency peaks with amplitudes up to 2600 Nm, which corresponds to local performance peaks of 460 kW per wheel at a velocity of 400 km/h. However, the predesign of the traction motors considers only a nominal power of 260 kW to be installed per wheel at the intermediate waggons. At a speed of 400 km/h, the main part of the installed power (75%) is needed to overcome the assumed running resistance, the remaining 25% are needed for acceleration or driving uphill.

In the following, the question is discussed, how the differential torques for the guidance task could be reduced to an acceptable value without a significant increase of the wheel wear. Hereby, the example of the NGT concept is utilised in order to gain insight into the design of a running gear with mechatronic guidance. Quantitative figures on properties and capabilities, significant parameters that rule the behaviour are in particular interesting. It is not the idea of the paper to present a read-to-use control set-up. Therefore, the main focus of the paper is the handling of the disturbances caused by track irregularities acting on a mechatronic track guidance system in a high-speed train. A further description of the DLR NGT project can be found in [2,9]. The vehicle model and its control scheme are described in Section 2. Section 3 includes an overview to the used optimisation tool. The influence of the track layout is analysed in Section 4. An improved controller that overcomes short-comings of the standard proportional-derivative (PD) controller is presented in Section 5. An outlook to the future work in this project is given together with the conclusions in Section 6.

## 2. Multi-body simulation models

### 2.1. *Vehicle model*

For the simulations with SIMPACK®, a shortened NGT unit comprising four intermediate cars and two end cars is used (Figure 1). Four intermediate wagons form a reasonable compromise. On the one hand, such a train unit enables investigations of the dynamic interactions between vehicles when inter-car dampers and the like are used, which are needed for improved running comfort. On the other hand, the computational costs are not unnecessarily increased.

The intermediate coaches consist of two running gears with one pair of IRW each and the car body (Figure 2(a)). An illustration of the running gear is shown in Figure 2(b). The wheels (1) of the running gear have a wheel radius of 0.625 m and are pivot-mounted on the opposite sides of the cranked beam (2). The primary springs (3) are stiff in the vertical direction and softer in the horizontal direction. At present, the primary springs are only defined by their stiffness (Table A2). The mechanical properties of the primary suspension are combined in

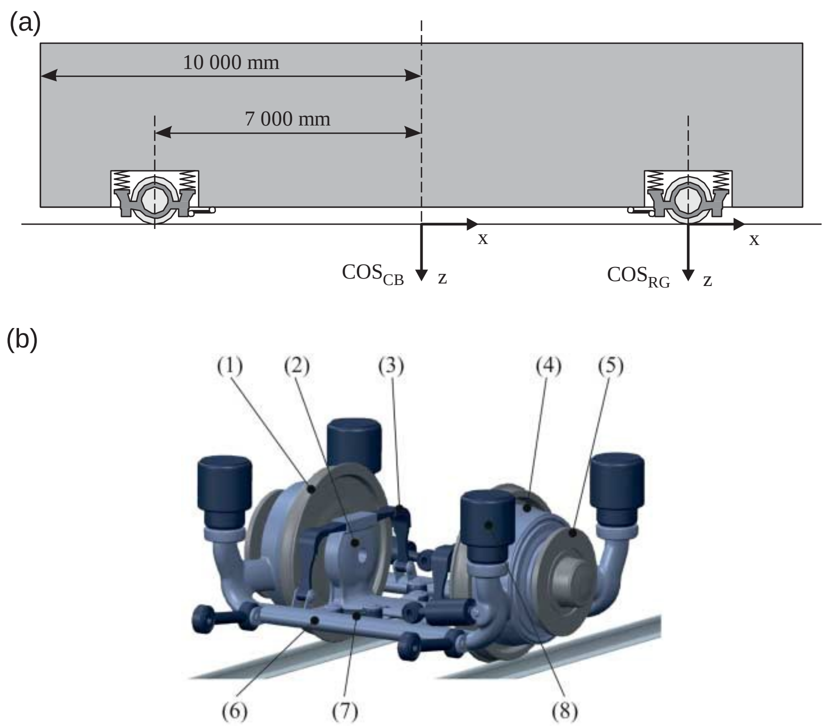


Figure 2. Multi-body-system (MBS)-structure of the NGT intermediate coach: (a) side view with co-ordinate systems; (b) running gear in detail.

one bushing element on each side and one central element. The final material (e.g. fibre-reinforced plastic composite) and design of the springs is not decided yet. The traction motor (4) and the brake discs (5) are arranged outside the wheels and are attached to the running gear frame (6) to reduce the unsprung mass. Inside the hollow shaft of the motor, a cardan shaft transfers the torque from the sprung motor to the wheel. Four levers (7) transmit the horizontal forces between the cranked beam and the running gear frame and define the centre for the steering rotation $\psi$. In addition to the secondary suspension (8), a lateral active centring and traction rods are needed. In the simulation model, an ideal power system is assumed and a controller (Section 2.3) is used for the calculation of the differential torques needed for the active guidance. If a differential torque is applied to both wheels, the axle beam rotates slightly around $\psi$: In consequence, the wheel pair moves in a lateral direction while running and compensates for a lateral excitation or force.

At the end wagon, two wheel pairs similar to those of the intermediate coaches are integrated into one bogie frame so that the train heads run on altogether four wheel pairs. The maximum axle load of all wheel pairs is 16 t. Apart from the active lateral centring and the mechatronic track-guidance, all other suspension elements are passive, but inter-car springs and dampers are introduced. After some variations of the control and suspension parameters, the NGT shows a good comfort performance.

## 2.2. *Track scenarios*

Three test tracks that approximately cover the spectrum of possible operational tracks are used for the simulation. Following an initial straight line, all three tracks contain an S-curve with intermediate straight sections and transitional curves (Figure 3 and Table A1). In addition Tracks 2 and 3 also contain a descending and ascending slope section. The slopes are added in order to create additional wear on the wheels from traction forces, although the driving resistance forces from the bearings and air resistance are neglected. Typical vertical, lateral and cross-level track irregularities are added for all track scenarios. The irregularities are generated using common PSD amplitude spectra, which are transformed into time domain

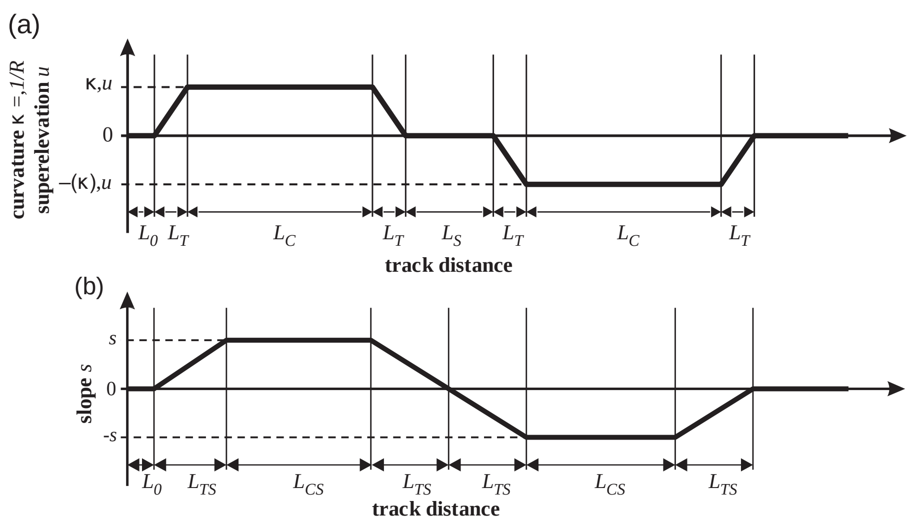


Figure 3. Layout of the test tracks: (a) curvature in horizontal plane; (b) inclination of vertical elevation.

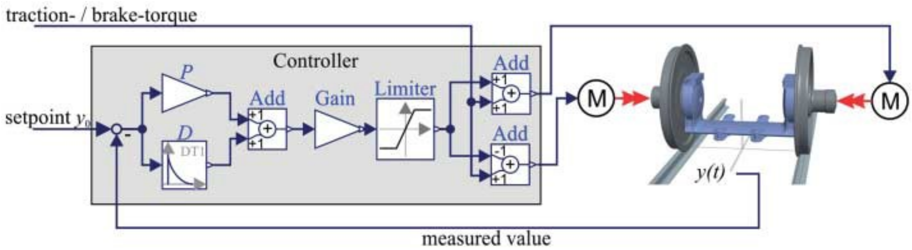


Figure 4. Principle of the mechatronic track guidance (with limiter).

with random phase shift. The track irregularities (ERRI high) represent a well maintained track for a velocity of 100 km⁄h.

Test Track 1 includes curves with a small radius that are typical for entering a station with several switches. The running velocity of 44 km⁄h is comparably low, but the small curve radius demands a high steering angle in the range of 47 mrad for perfect radial steering.

lines (Test Track 2). At curves with a radius of 600 m, the necessary steering angle decreases to 12 mrad, but the influence of track irregularities increases because of the higher speed of
100 km⁄h.

The NGT is designed for operation on high speed lines represented by Test Track 3. At a running velocity of 400 km⁄h, the track irregularities define the most serious challenge for the mechatronic track guidance. For Test Track 3, the irregularities generated using common PSD spectra are modified in order to meet the demands regarding the tracks for the acceptance test in EN 14363 App. C [10] – with an extrapolation to 400 km⁄h.

### 2.3. *Control scheme*

In this state, an ideal, simple PD-controller is used for the track guidance in order to understand the system and the influencing parameters and to have a benchmark for the future development of sophisticated controllers. Figure 4 shows the layout of the control scheme: The control is based on the measurement $y(t)$ of the instantaneous distance between the centre of the wheel pair and the virtual track centreline in the middle of the right and left rail. Possible sensors are discussed in [2] and are a current research topic at DLR.

The lateral displacement of the axle with respect to the central position between both rails $y(t)$ is the relevant sensor information here provided by the MBS during simulation. This measured distance is fed back and compared to the set-point, which is defined to be zero. The controller only contains a proportional and differential term. An additional integral term does not lead to relevant improvements of the control performance because the system itself exposes integrating behaviour. The actuation quantities of the control are the torques; the same absolute values are applied to the right and the left wheel but with an alternating sign. Finally, the demanded traction or brake torque generated in the speed control of the vehicle model is added. Therefore, the speed control compares the current velocity and position of the vehicle with the desired values. This guarantees nearly constant running speed during the simulation.

In a second step – after the optimisation of only the controller parameters, $P$ and $D$ does not deliver satisfying results for the needed torque (Section 3.2) – the limiter for the torque after the gain $k$ in Figure 4 is introduced (Section 5). The quality of the mechatronic track guidance is mainly influenced by the control parameters $P$ and $D$, but also by the rotational stiffness and damping in the primary suspension and the mass and inertia of the wheels. If it exists, the limiter also affects the steering quality. The rotational stiffness and damping can be tuned by the levers and the longitudinal properties of the leaf spring.

## 3. Optimisation

### 3.1. *Set up of the optimisation loop*

Multi-body simulations of the NGT running dynamics are performed using several control set-ups including an actuation limitation. The simulation scenarios for the optimisation are orientated at the three test tracks. In order to reduce the computation effort, only one vehicle (coach or end wagon) runs on a shortened track section. Figure 5 contains the results of a typical simulation run for the optimisation: At 400 km/h, the vehicle runs from a straight track, passing a right-hand curve with 8500 m radius and transition curves (Figure 5(c)). The simulated time is 20 s. In Figure 5(a), the transient differential torque that is applied by the PD-control is shown. The lateral position of the wheel pair centre is shown in Figure 5(b)

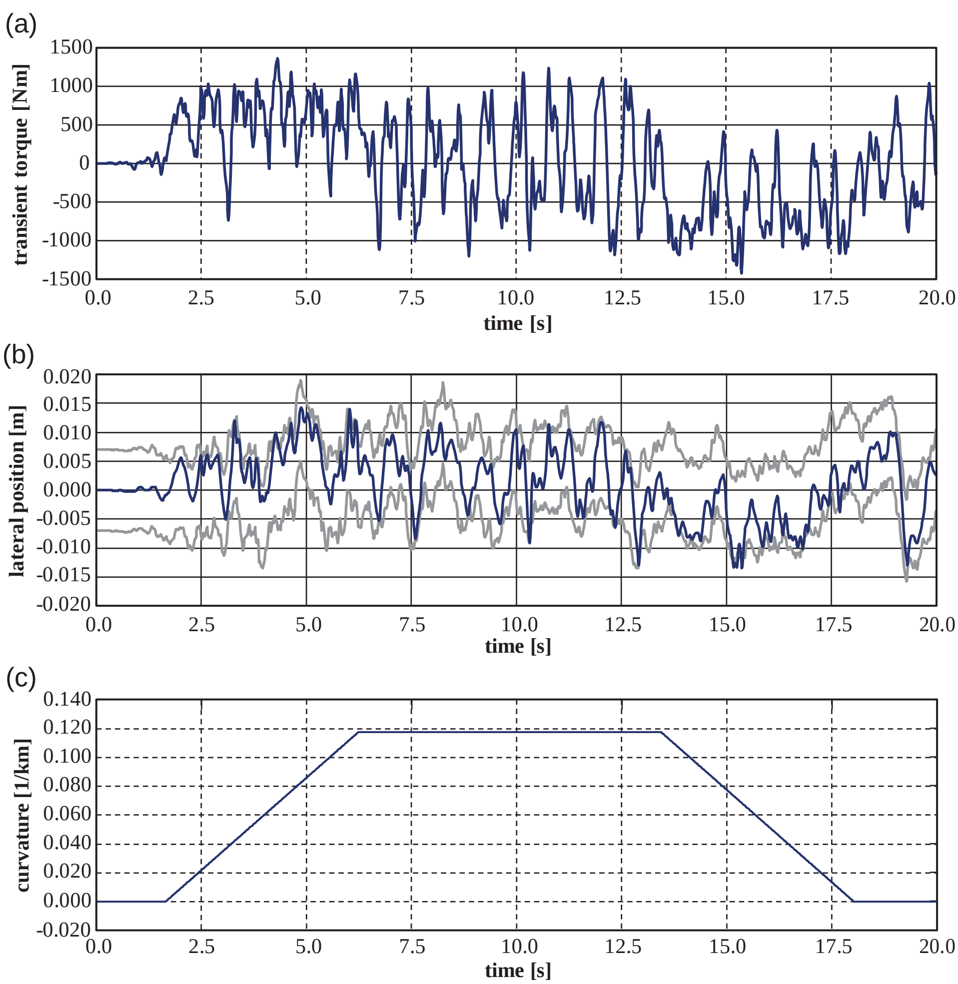


Figure 5. Results of a typical simulation run for the optimisation: (a) transient torques; (b) lateral position of wheel pair within the gauge clearance moved by lateral irregularities; (c) track curvature.

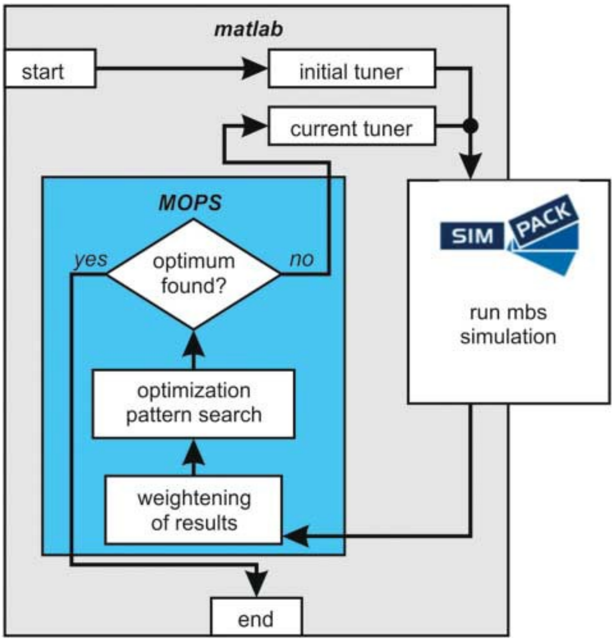

Figure 6. Set up of the optimisation loop.

together with the lateral track irregularities in grey, which are drawn in the distance of the gauge clearance. This diagram is in particular well-suited to simultaneously observe both, the deviation of the wheel pair from the desired central position and flange contact events.

Assuming a low influence of the control system on the running comfort, it is possible to optimise the control system at a single vehicle. Afterwards the behaviour of the single vehicles in the train set is checked in a whole train simulation (Section 5).

The parameter sets of the controllers are optimised using computer-aided optimisation. The tuneable parameters are the proportional part $P$ and the differential part $D$ in the controller as well as the rotational stiffness $c_t$ and the rotational damping $d_t$ (Table A2). The simulations are performed with the multi-body code SIMPACK®. The optimisation tool used to determine the control parameters is the MATLAB®-based DLR in-house tool MOPS,[11] which is an environment for the multi-objective-multi-parameter synthesis. Multi-objective parameter synthesis is based on algorithmic parameter tuning with nonlinear programming or evolutionary computation, combined with system model simulations with high accurateness. MOPS and SIMPACK® are invoked in loops by MATLAB® as the framework master. The optimisation run is started in Matlab® with the initial tuner (Figure 6). Matlab® starts the SIMPACK® multi-body simulation and receives the essential results. Afterwards MOPS weighs the results and executes the optimisation with the Pattern Search approach.[12] Pattern Search is a derivative-free method and uses only criteria evaluations. MOPS enables to find a Pareto-optimal solution for the set of parameters taken in SIMPACK®.

In a first optimisation run, the mechanical parameters of the running gear – the torsional stiffness and damping – show a small sensitivity, if the stiffness is rather low and the damping is rather high. Therefore, both parameters are constant in the following optimisation of the control parameters $P$ and $D$.

The objectives are defined by the drive power torque and the wheel wear (multi objective optimisation). In the optimisation, specific wheel wear values shall be achieved with the lowest possible drive torque. In order to meet the NGT project targets, the wear must be lower than 80% of the values of the reference vehicle.

As a simplification in the optimisation loop, the material volume at the wheel removed by wear is assumed to be proportional to the work done by friction forces. The friction work $w_{\mathrm{f}}$ is defined as the integral of the product of tangential forces $T_i$ and creep velocity $v_i$ within the rail–wheel contact (1).

$$w_{\mathrm{f}} = 0.5 \int |T_x v_x| + |T_y v_y| \,\mathrm{d}t. \tag{1}$$

A reference vehicle representing a typical conventional high-speed vehicle is used in order to evaluate a reference quantity specifying the wear. This vehicle has the same axle load and powered bogies with conventional wheelsets. The friction work in the course of the simulation period with the reference vehicle is taken to quantify the performance of the controller in the NGT.

### 3.2. *Optimisation results*

The optimisation of the control parameters exposes a design conflict. Wear reduction is only possible if sufficiently high actuation torque values are provided for the control task: Figure 7(a) presents the maximum applied torques as a function of the wear for all three test tracks. Each point is the result of one optimisation run and indicates the best solution with the lowest differential torque for a given wear value. The wear is specified relative to the wear of the conventional reference vehicle. The dependency between wheel wear and differential torque can be clearly seen. At Test Track 3, it is possible to get wear rates up to 70% with respect to the reference vehicle without a significant increase of the differential torque, whereas lower wear rates are only possible with much higher torques. The results for both other test tracks are similar. The highest torque values are needed on Test Track 1. However, this case is less critical because the motor is able to provide these high torque values at low speeds.

For further interpretation, it is helpful to convert the differential torque into the equivalent power with respect to the running velocity (Figure 7(b)). At Test Track 1, the required power is comparable low. Although the results for Test Track 3 are calculated with an optimised control system, the necessary power to provide the differential torque is in the range of the power rate of 260 kW of the given traction motor, which is mainly needed for traction tasks. In order to meet the NGT project goal of 20% wear reduction, a maximum torque of approximately 1200 Nm had to be applied at Test Track 3. Otherwise, more than 60% wear reduction is possible with 1775 Nm maximum torque. In comparison to the initial situation, it is possible to meet the wear reduction with lower drive torque but the torque is still over the available torque.

The development of the differential torques for the case Test Track 3 with 1400 N/m (250 kW) and 53% wear in Figure 7 are shown in Figure 5. Fortunately the high torque values are only short peaks. Therefore it seems to be a reasonable assumption that a peak power of 50% of the nominal motor power can be allowed for guidance tasks at this velocity, which is equivalent to a power limit of 130 kW. However, it is not possible to achieve the second objective of the wheel wear (work of friction) lower than 80% relative to the reference vehicle with a maximum peak power of 130 kW at Test Track 3. It is obvious, that there is a trade-off between both objectives, which cannot be solved with the used controller at Test Track 3. At the other two test tracks both objectives can be satisfied simultaneously. In order to discuss the influencing factors of the track, the results in the time domain are analysed in the next section.

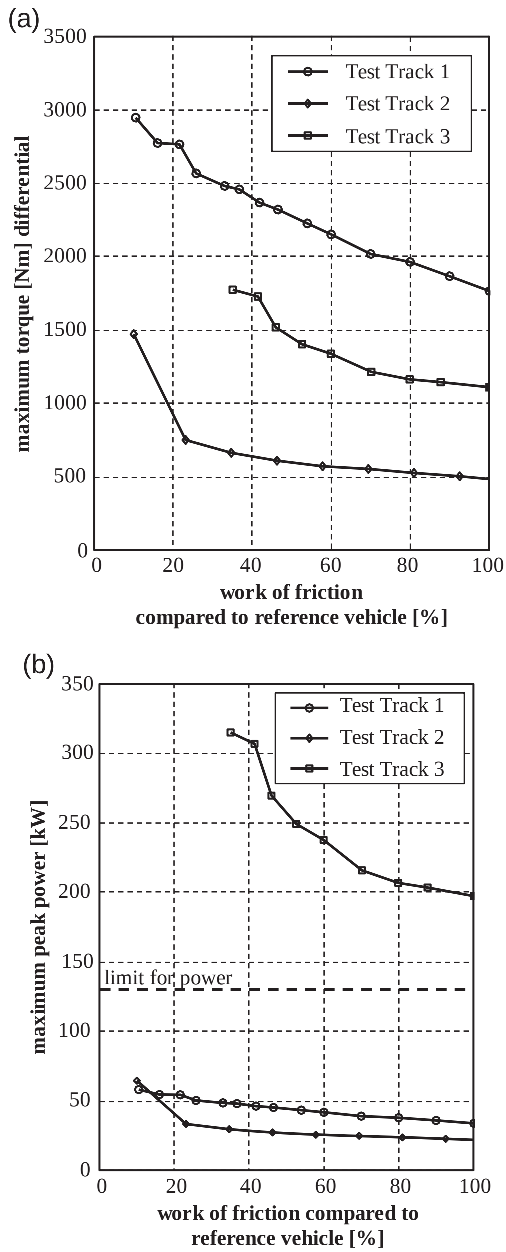


Figure 7. Pareto front of the conflicting optimisation goals: (a) actuation torque versus friction work; (b) and actuation power versus friction work.

## 4. Influence of the track properties on the actuator requirements

### 4.1. *Influence of line layout*

Figure 5 shows the transient torques that are applied by the PD-control and are necessary to get 47% wear reduction compared to the reference vehicle. The torques in the top plot exhibit a high mean value of 600 Nm during the time period from 1.8 to 6.4 s in which the running

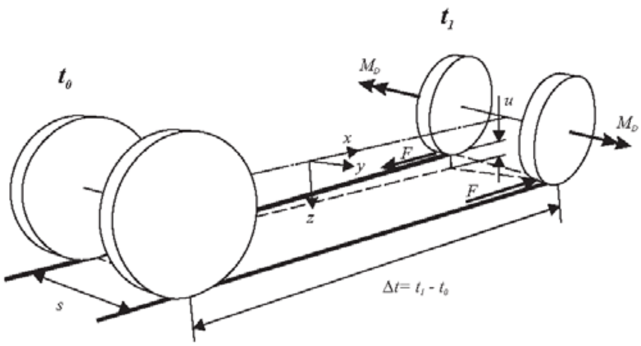


Figure 8. Sketch of the Minimal Model and numerical values to re-evaluate the drive torque during transition curve.

Table 1. Parameter of minimal model

| *Parameter* | *Symbol* | *Unit* | *Value* |
|---|---|---|---|
| Super elevation at the end of transition curve | $u$ | [m] | 0.170 |
| Wheel base | $s$ | [m] | 1.500 |
| Rolling radius | $r$ | [m] | 0.625 |
| Wheel inertia | $\Theta_{yy}$ | [kgm²] | 348 |
| Duration passing transition curve | $\Delta t$ | [s] | 4.59 |
| Running speed | $v$ | [m/s] | 111.1 |
| Angular speed around x | $\omega_x = \frac{u}{s\,\Delta t}$ | [rad/s] | 0.0247 |
| Angular speed around y | $\omega_y = -\frac{v}{r}$ | [rad/s] | -177.78 |

gear passes the transition curve (Figure 5(c)) and the lateral position of the running gear, shown in Figure 5(b), tends to run near the inner rail side. Additional simulations showed that this mean torque value is nearly independent of the rotational stiffness or damping at the axle beam. During this time period, the running gear rotates around the longitudinal vehicle axis due to the super elevation. It is assumed that the particular high torque values during this period compared to the torques needed to run through the constant radius curve are related to gyroscopic effects.

In order to substantiate this statement, the Minimal Model in Figure 8 presents a system consisting of the two wheels with the inertia tensor rotating around the $y$-axis with constant rotational velocity $\omega_y$ due to the rolling of the wheels along the rails. While approaching the transition curve, the wheels are additionally rotated around the $x$-axis due to the super elevation ramp of the track so that a small but non-vanishing rotational velocity $\omega_x$ is given (Table 1). If Euler's angular momentum law is resolved with respect to a sliding coordinate system that does not perform the overturning motion of the wheels, see (4.66) in [13] and acceleration terms are neglected; the relationship for the torque $M_z$ in Equation (2) can be derived. The angular velocity of the wheel $\omega_w$ is given in Equation (3) and the angular velocity of the coordinate system $\omega_c$ in Equation (4).

$$\vec{M} = \Theta\,\dot{\vec{\omega}}_w + \vec{\omega}_c \times \Theta\,\vec{\omega}_w, \tag{2}$$

$$\vec{\omega}_w = \begin{pmatrix} \omega_x \\ \omega_y \\ \omega_z \end{pmatrix}, \quad \dot{\vec{\omega}}_w \approx \vec{0}, \tag{3}$$

$$\vec{\omega}_c = \begin{pmatrix} \omega_x \\ 0 \\ \omega_z \end{pmatrix}. \tag{4}$$

The vector $M$ of the external torques in Equation (5) contains a torque $M_x$ caused be vertical wheel and spring forces, which does not influence the driving torques. The two applied traction torques $M_D$ around the $y$-axis sum up to zero:

$$\vec{M} = \begin{pmatrix} M_x \\ 0 \\ -Fs \end{pmatrix}, \tag{5}$$

$$\Rightarrow \; M_z \approx \; \omega_x \, \omega_y \, \Theta_{yy} = F \, s \;\; . \tag{6}$$

$M_z$ is a result of the longitudinal traction forces $F$ that are applied twice but with the distance $s$ that follows from the tape circle gauge of the wheels (6). The force $F$ multiplied by the wheel radius $r$ yields the torque $M_D$ applied by each traction drive, i.e. $M_D = -Fr$ :

$$M_D = \frac{\omega_x \omega_y \Theta_{yy}}{s} \; r = \; -633 \text{ Nm} \; . \tag{7}$$

Compared to the transient torques in Figure 5(c) in the time interval from 1.8 to 6.4 s this value seems to be slightly overestimated, but nevertheless provides a reasonable explanation for the characteristics. In addition, it can be stated that the relevant design parameter to influence the actuation torques in transition curves is the inertia term $_{yy}$ of the wheels.

With a positive $\omega_x$ and a negative $\omega_y$ the torque $M_z$ in Equation (6) is negative, which means it prevents a rotation in the positive direction. Without any countermeasure, the wheel pair has a tendency to over-steer and will stick at the inner rail. As Figure 5(b) shows, the guiding system is able to steer the wheel away from flange contact.

Usually the influence of gyroscopic effect on the running dynamics of a wheelset is very low in comparison to other effects; therefore this is a surprising result. Of course, in this case several reasons amplify the effect: IRWs are used, which are more sensitive to disturbing effects. Furthermore, the wheels of the NGT have a comparably large diameter and therefore a high inertia. At last, the super elevation of 170 mm is quite high but not unusual for pure passenger high speed lines with ballastless track. However, the design of the transition curve as part of the line layout determines also the requirements for the actuators.

### 4.2. *Influence of track irregularities*

The influence of the track irregularities can be observed in Figure 5 between 6.4 and 13.4 s. This time interval is associated with stationary running conditions through a curve with constant radius and with 8500 m radius as well. Because of the high radius and the high super elevation in combination with of the ability of the radial steering, the conditions are nearly the same as on a straight track. During this time period, the torque is excited by the random track irregularities – especially in the lateral direction and cross level. The oscillation of the differential torque is directly related to the lateral track irregularities. The lateral motion in the centre plot in Figure 5 shows similarities to the hunting motion of a classical wheelset. Sometimes the wheel flanges hit the rails. However, the performance is better in comparison to the reference vehicle with bogies. This behaviour is important for a uniform wear distribution on the wheel in the lateral direction.

At maximum, a peak torque of 1200 Nm that corresponds to 215 kW is needed for the handling of track irregularities. Compared with the limit value discussed before, this value is still too high. However, the optimisation offers no better results: even allowing moderate higher wear, the torque stays on the same high level (Figure 7).

## 5. Results with improved controller

The optimisation of the control parameter presented in Section 3 does not enable the necessary reduction of the differential torques. Of course, smaller wheels with lower inertia can be a solution, also at straight tracks. Because the maximum values occur as short peaks (Figure 5(a)) a second solution is suggested: Will it be possible to limit the maximum torque without a significant increase of the wheel wear?

At first, the initial control parameters, which represent a wear reduction of 47%, were used for the parameter variation with subsequently reduced limit values. Therefore, the limiter block in the control system (Figure 4) is activated. Figure 9 depicts the applied torques obtained that way as a function of time. The maximum applied torque was reduced from 1400 Nm (without limitation) down to 600 Nm. For a limitation of 1000 Nm, no significant influence on the running dynamics can be seen. A further limitation, especially of 600 Nm, results in a different behaviour in the transition curve, which may increase the wear of the wheels. However, the first and very important result is that such a reduction does not destabilise the control set-up. In principle, the control works even with a 500 Nm maximum actuation effort. Though, it is to be expected that such a reduction promotes flange contact events and causes a significant more wear.

As the curve with circles in Figure 10 demonstrates, this expectation is met, but surprisingly an increase of wear only occurs if the maximum torque is limited below 750 Nm. Even with a maximum torque of 700 Nm, the wear increases to 125% referred to the situation without limitation and stays 20% below wear of the reference vehicle. However, the limiter completely changes the behaviour of the control-system. Therefore, it is not sure that the used control parameters are the best set-up.

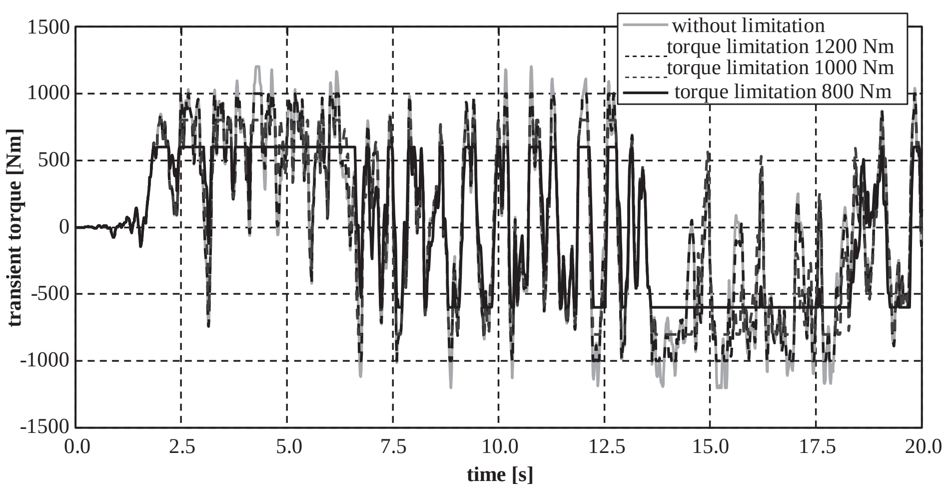


Figure 9. Plot of drive torques with subsequently reduced limitation values.

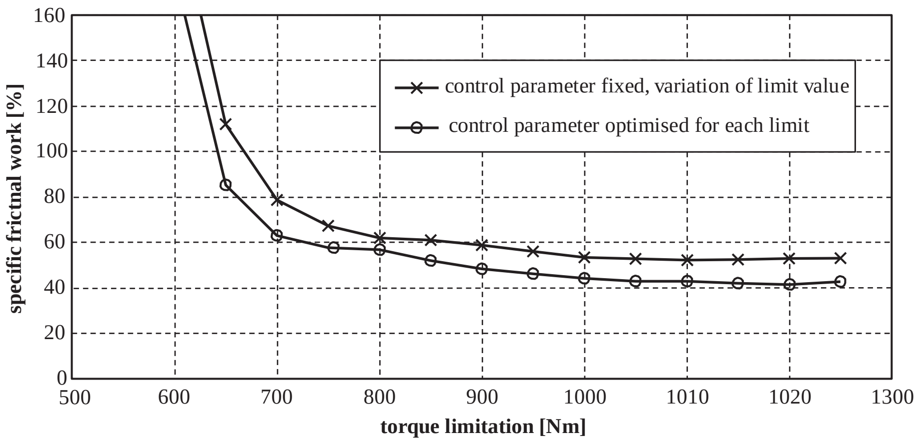


Figure 10. Relation of wear reduction versus torque limitation values.

Table 2. Frictional power, drive torque and power for the three scenarios

| *Parameter* | *Symbol* | *Unit* | | *Scenario:* | |
|---|---|---|---|---|---|
| | | | *Test Track 1* | *Test Track 2* | *Test Track 3* |
| Frictional work per length (reference vehicle) | $w_{ref}$ | [Nm/m] | 108.5 | 26.3 | 3.84 |
| Frictional work per length (NGT) | $w_{NGT}$ | [Nm/m] | 35.6 | 16.5 | 2.27 |
| Spec. Frictional work NGT | $w_{NGT}/w_{ref}$ | [%] | 33% | 62% | 59% |
| Max. peak value torque (steering) | $M_{max}$ | [Nm] | 3000 | 650 | 700 |
| RMS. value torque (steering) | $M_{rms}$ | [Nm] | 1567 | 398 | 594 |
| Max. peak value power (steering) | $P_{max}$ | [kW] | 58.7 | 28.9 | 124.4 |
| RMS. value power (steering) | $P_{rms}$ | [kW] | 7.8 | 17.7 | 105.7 |
| Controller parameter | $D$ | [Nms/m] | 6.85 | 0.208 | 17.5 |
| Controller parameter | $P$ | [Nm/m] | 356950 | 78292 | 332900 |

In a second loop, the control system with a limiter is optimised again with different limitation values. For each specific limitation value, the optimal control parameters $P$ and $D$ are searched. In this case, a single objective (lowest wear) optimisation is possible, because of the defined torque limit. The curve with crosses in Figure 10 shows the results for this optimisation, which are slightly better than the results of the variation of the limit values with fixed control parameters. A reasonable limitation value for the drive torque is 700 Nm. In this case, both targets are fulfilled: the maximum peak power is 125 kW and a wear reduction of more than 35% compared to the reference vehicle is possible. The corresponding control parameters are listed in Table 2. In general, a high rotational damping and a low rotational stiffness parallel to the steering degree of freedom have a positive effect (central bushing in Table A2).

Similar optimisations are executed for both other test tracks and the behaviour is finally verified by whole train simulations over the longer distance with optimised parameters and the limitation of the maximum torque. A good compromise is achieved: the maximum control effort can be reduced to 700 Nm also enabling a 59% wear reduction of the NGT compared to the reference vehicle (Table 2). Similar to Figure 9, only in transition curves the maximum steering torque is continuously needed for of few seconds. All other peaks occur with oscillating signs; therefore the mean power is nearly zero.

Table 2 and Figure 11 compare the results of the simulated runs on the three test tracks over the full length. Because of the nonlinear behaviour of the wheel–rail contact, the values of frictional work slightly different compared to the simulations on the shortened sections. As mentioned before, the frictional work is only a simplified criterion for the wear. Using the

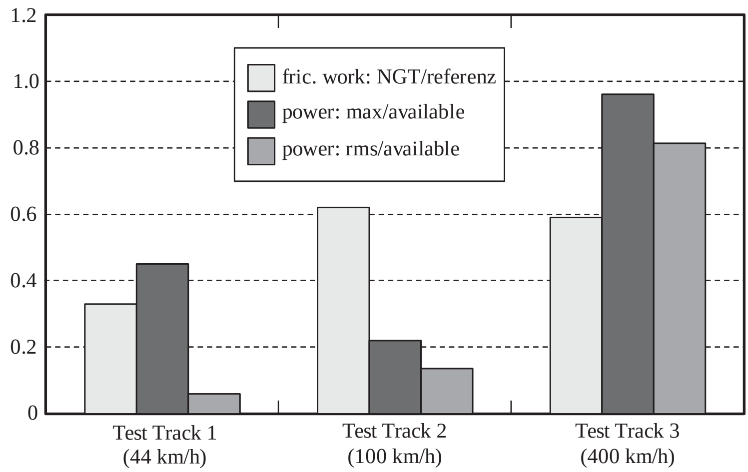


Figure 11. Comparison of the wheel wear and needed motor power at the three test tracks.

knowledge of the geometry of the contact-patch and wear law [14,15], the quantity of removed material and the shape of the worn wheel and rail profiles can be calculated. In total, a reduction of the frictional work between 38% and 67% is possible. The peak torque values stay below the velocity depending limits. Test Track 3 demands the highest motor performance. At the other two test tracks the power requirements are much lower. With optimised parameters and the limitation of the maximum torque, it is possible to run with overload peaks within the given limit.

Although the rms-values of the power are high, it must be noted that the mean value per axle is zero since the control effort power applied to the right wheel is equal but opposite to the control power applied to the left wheel. Summing up both sides, the track guidance system consumes no or nearly no additional power. Consider an additional traction effort, the controller only changes the distribution of the traction power on both wheels with respect to the demanded differential torque. If no traction forces are needed, the motor at one wheel, which has to brake, generates the power for the other motor which has to accelerate.

Nevertheless, the values written in Table 2 are important lay-out quantities of the traction motors, since these values are to be supplied by each individual motor.

## 6. Conclusions and outlook

The activities that are built upon the lay-out of the NGT running dynamics are presented. In order to organise the guiding task and improve the dynamic behaviour of the running gears, multi-body simulations of the NGT running dynamics have been performed using several control set-ups. The parameter sets of the controllers have been optimised using computer-aided optimisation.

The optimisation of the control parameters exposes a design conflict. Wear reduction is only possible if sufficiently high actuation torque values are provided for the control task. However, it is not possible to solve this conflict satisfactory only with a PD controller. Therefore a PD controller with a actuation limitation is proposed. Regarding the current NGT configuration, the supply of 700 Nm as the maximum control effort is a good compromise, since it enables between 38% and 67% wear reduction of the NGT compared to the reference vehicle.

The actuator performance is mainly influenced by the track irregularities as well as the line layout. The maximum torque values are required to get the running gear through the transition curves at the entrance and the exit of the curves. This behaviour can be explained by gyroscopic effects due to the inertia of the fast rotating wheels. From this point of view, it is proposed to reduce the inertia of the wheels (e.g. by reduced wheel radius), since this leads to lower actuation efforts.

Further investigations will be performed in order to improve the understanding of the dynamic behaviour of the controlled running gear, with the development of a universal controller and the proof of its stability. It is to be evaluated which refinements are to be achieved by the introduction of a feed-forward component to the control set-up. In this way, information from leading running gears or from the knowledge of the track routing may be exploited to get a better performance. In parallel, a sensor concept is developed and tested at the DLR 1:5 roller rig and considerations regarding a fall-back strategy are made.

## References


[1] Goodall RM, Bruni S, Mei TX. Concepts and prospects for actively controlled railway running gear. Veh Syst Dyn. 2006;44:60–70.
[2] Kurzeck B, Valente L. Design aspects of a mechatronic track guidance. 22nd Symposium on Dynamics of Vehicles on Roads and Tracks, Manchester Metropolitan University, UK, 2011.
[3] Perez J, Busturia JM, Mei TX, Vinolas J. Combined active steering and traction for mechatronic bogie vehicles with independently rotating wheels. Ann Rev Control. 2004;28:207–217.
[4] Bruni S, Goodall RM, Mei TX, Tsunashima H. Control and monitoring for railway vehicle dynamics. Veh Syst Dyn. 2007;45:743–779.
[5] Gretzschel M, Bose L. A mechatronic approach for active influence on railway vehicle running behaviour. Veh Syst Dyn. 1999;33:481–430.
[6] Mei TX, Qu KW, Whitley M. Control of wheel motors for the provision of tight rail traction and steering. UKACC International Conference on Control, Coventry University, UK, 2010.
[7] Schade S, Hermanns M, Dellmann A. Mechatronic control for independently rotating railway wheelsets. ZEVrail. 2010;134:404–410.
[8] Liang B, Iwnicki SD. Independently rotating wheels with induction motors for high-speed trains. J Control Sci Eng. 2011;Article ID 968286, 10 pages.
[9] Winter J. (Coordinator). NGT – Next Generation Train. Rail Technol Rev. Special Issue, 2011.
[10] EN 14363. Railway applications – testing for the acceptance of running charactersitics of railway vehicles – testing of running behaviour and stationary tests, German Version EN 14363:2005.
[11] Joos H-D, Bals J, Looye G, Schnepper K, Varga A. A multi-objective optimisation-based software environment for control systems design. IEEE International Conference on Control Applications and International Symposium on Computer Aided Control Systems Design, Glasgow, Scotland, UK, 2002.
[12] Hooke R, Jeeves TA. Direct search solution of numerical and statistical problems. J ACM. 1961;8:221–229.
[13] Meirovitch L. Methods of analytical dynamics. New York: McGraw-Hill Inc., 1970.
[14] Archard J. Contact and rubbing of flat surfaces. J Appl Phys. 1953;24:981–988.
[15] Pearce T. Prediction of wheel profile wear. WEAR. 1991;144:343–351.

## Appendix

Table A1. Track parameter

| *Parameter* | *Symbol* | *Unit* | *Scenario:* Test Track 1 | *Test Track 2* | *Test Track 3* |
|---|---|---|---|---|---|
| Speed | $v$ | [km/h] | 44 | 100 | 400 |
| Curve radius | $R$ | [m] | 150 | 600 | 8500 |
| Super elevation | $u$ | [mm] | 0 | 120 | 170 |
| Slope | $s$ | [%] | - | 1 | 1 |
| Initial length | $L_0$ | [m] | 140 | 240 | 260 |
| Length transition curve | $L_T$ | [m] | 30 | 90 | 510 |
| Length constant curve | $L_C$ | [m] | 200 | 1000 | 3000 |
| Length intermediate straight | $L_S$ | [m] | 20 | 400 | 1350 |
| Length slope transition | $L_{TS}$ | [m] | - | 25 | 1200 |
| Length constant slope | $L_{CS}$ | [m] | - | 1355 | 2295 |
| Track irregularities | | | ERRI high | ERRI high | conform to EN 14363 |
| Simulated time | | [s] | 60 | 120 | 100 |
| Percentage of total running distance | | [%] | 3 | 7 | 90 |

Table A2. Vehicle parameters (intermediate coach)

| *Parameter* | *Symbol* | *Definition* | *Value* | *Unit* |
|---|---|---|---|---|
| carbody | $m_{cb}$ | Mass of carbody | 24054 | kg |
| | $I_{cbx}$ | Roll moment of inertia | 68000 | kgm² |
| | $I_{cbx}$ | Pitch moment of inertia | 797000 | kgm² |
| | $I_{cbx}$ | Yaw moment of inertia | 787000 | kgm² |
| | $z_{cg,cb}$ | Vertical position centre of gravity | -2.051 | m |
| running gear frame | $m_{rg}$ | Mass of running gear frame | 2417 | kg |
| | $I_{rgx}$ | Roll moment of inertia | 2517 | kgm² |
| | $I_{rgx}$ | Pitch moment of inertia | 291.4 | kgm² |
| | $I_{rgx}$ | Yaw moment of inertia | 2627 | kgm² |
| | $z_{cg,rg}$ | Vertical position centre of gravity | -0.585 | m |
| axle beam | $m_a$ | Mass of axle beam | 372 | kg |
| | $I_{ax}$ | Roll moment of inertia | 166.7 | kgm² |
| | $I_{ax}$ | Pitch moment of inertia | 8.7 | kgm² |
| | $I_{ax}$ | Yaw moment of inertia | 166.7 | kgm² |
| | $z_{cg,a}$ | Vertical position centre of gravity | -0.553 | m |
| wheel | $m_w$ | Mass of wheel | 592 | kg |
| | $I_{wx}$ | Roll moment of inertia | 71.8 | kgm² |
| | $I_{wx}$ | Pitch moment of inertia | 174.0 | kgm² |
| | $I_{wx}$ | Yaw moment of inertia | 71.8 | kgm² |
| | $y_{cg,w}$ | Lateral possition centre of gravity | ± 0.897 | m |
| | $z_{cg,w}$ | Vertical position centre of gravity | -0.625 | m |
| Primary suspension sidewise bushing | | Position in y | ± 1.000 | N/m |
| | | Stiffness in y | 1e7 | N/m m |
| | | Stiffness in z | 2e6 | N/m m |
| | | Stiffness in around y | 8e6 | Nm/rad |
| | | Damping in y | 137000 | Ns/m |
| | | Damping in z | 61100 | Ns/m |
| | | Damping in around y | 30000 | Nms/rad |
| Primary suspension central bushing | $c_t$ | Stiffness in around z | 1e3 | Ns/m |
| | $d_t$ | Damping in around z | 3e5 | Nms/rad |